Improvement of Rigidity for Rubber-Toughened Polypropylene via Localization of Carbon Nanotubes

Rujirek Wiwattananukul, Bowen Fan, and Masayuki Yamaguchi*

School of Materials Science, Japan Advanced Institute of Science and Technology

1-1 Asahidai, Nomi, Ishikawa 923-1292 JAPAN

*Corresponding author. E-mail address: m_yama@jaist.ac.jp (Masayuki Yamaguchi)

Phone: +81-761-51-1621

Fax: +81-761-51-1149

ABSTRACT

A methodology for controlling the localization of multi-walled carbon nanotubes (MWCNTs) was studied using an immiscible polymer blend composed of isotactic polypropylene (PP) and ethylene-co-propylene rubber (EPR). We found that the MWCNTs were localized in EPR domains within the composite, which was prepared at 280 °C. EPR molecules bonded to the MWCNT surface are responsible for the localization in EPR. Conversely, MWCNTs preferentially resided in the matrix when the composite was prepared at 190 °C along with nitrogen gas purging. Because of the selective localization of the MWCNTs in the matrix, the composite obtained via mixing at the lower temperature exhibited a higher Young's modulus and yield strength. These findings demonstrate that mixing conditions greatly affect the MWCNT distribution and thus the mechanical properties of PP/EPR blends.

Keywords: Carbon nanotubes; Polymer-matrix composites; Mechanical properties; Mixing

1. Introduction

Carbon nanotubes (CNTs) have received much attention in both academia and industry and are recognized as being suitable candidates for use as fillers for thermoplastic and thermosetting resins to enhance their Young's modulus and strength effectively; thus, their range of potential applications can be significantly expanded [1–3]. In the case of immiscible polymer blends with phase-separated structures, the selective localization of CNTs in one of polymer phases or at the interface is crucial to achieve a material with tailored properties [4–6]. For example, the rigidity and electrical conductivity can be efficiently enhanced when CNTs are selectively dispersed in a continuous phase of a blend with a sea-island structure. The migration of fillers to a favored polymer phase during mixing usually occurs when fillers are pre-dispersed in a thermodynamically unfavorable polymer [4,6,7]. Moreover, processing conditions and/or mixing protocols can have a significant impact on the final morphology [4,8,9]. Furthermore, it was reported that the addition of multi-walled carbon nanotubes (MWCNTs) can change the domain sizes of a phase separated polymer blend, leading to the modification of its electrical and mechanical properties [9–11].

Isotactic polypropylene (PP) with an impact modifier such as ethylene-co-propylene rubber (EPR) is widely employed in industry because of its excellent balance of both rigidity and toughness [12–15]. Recently, however, the demand to enhance polymer rigidity is increasing, especially for automobile applications, so that the thickness and weight of the polymer components can be reduced. Hence, the focus on MWCNT additives is based on wanting to improve a polymer's rigidity. For the above mentioned polymer composites, fillers have to be localized in a continuous phase to effectively increase the rigidity without loss of impact strength [16]. It has been reported that carbon nanofillers, such as carbon black (CB), vapor-grown carbon fibers (VGCFs) and CNTs, tend to reside in polyethylene (PE) and ethylene copolymers in an immiscible blend, although the interfacial tension between PE and

carbon nanofillers is high. Sumita et al. found that CB preferentially localized in the PE phase in blends of PE and PMMA [17,18]. Wu et al. also reported that VGCFs were dispersed in PE in PE/PMMA blends. They proposed the concept of an "entropy penalty" that causes a selective adsorption of PE chains on the rough ends of VGCF owing to the flexibility of polymer chains, which leads to a self-assembled conductive network within the PMMA matrix. Even in a blend with another polyolefin, such as PP, CB was found to be selectively located in the blend's PE phase [19–22]. Haddadi-Asl studied the structure and properties of PP/EPR blends containing both CB and graphite fibers. He found that most conductive carbon fillers resided in the EPR phase, resulting in a low proportion of fillers in the PP phase [23]. Hemmati et al. studied the effect of the concentration of both single-walled carbon nanotubes (SWCNTs) and their compatibilizer in PP, i.e., PP-graft-maleic anhydride (PP-g-MA), on the morphology and mechanical properties of PP/ethylene-propylene-diene terpolymer (EPDM) blends. They reported that the tensile modulus was greatly enhanced by increasing the SWCNT content; this enhancement was more pronounced in the compatibilized composite. Furthermore, EPDM was uniformly distributed in the PP matrix with low concentrations of the SWCNTs and compatibilizer. However, the distribution of EPDM was not homogeneous with an increased filler concentration because the concentration of PP-g-MA in the matrix was also increased, thereby leading to a reduction of matrix viscosity. As a result, the viscosity ratio of EPDM to PP was increased and thus the break-up process of the EPDM droplets became more difficult [24].

The localization of CNTs in the matrix is also a key technology for realizing electro-conductive composites. Meincke et al. showed that the selective localization of CNTs in polyamide-6 in a blend of polyamide-6 and acrylonitrile-butadiene-styrene terpolymer greatly reduced the concentration of CNTs required to form a conductive network [25]. Phromdee et al. found that the volume resistivity of a PP/EPR blend with CBs was low compared with that

of a CB-filled PP homopolymer because of double percolation, which involves CBs creating a conductive path in the continuous sections of the EPR phase [26].

In our previous papers, we revealed that an interphase transfer of the MWCNTs from PP or PE to polycarbonate (PC) occurs during the annealing of laminated sheets composed of PP/MWCNT or PE/MWCNT and PC. However, such a transfer was not detected at all from PC to PP or PE. This is reasonable because the interfacial tension between PC and MWCNTs is lower than that between polyolefin and MWCNTs. In contrast, MWCNTs prefer to move from PC to PE during mixing at high temperature. It was revealed that this phenomenon occurs owing to the adsorption of PE molecules on the surface of the MWCNTs. Furthermore, the adsorption of PE is pronounced owing to the presence of oxygen during mixing at high temperature [6,27]. The reaction between oxygen and the ethylene unit, which produces polymer radicals, is responsible for the surface adsorption; thus, a similar phenomenon is expected to occur for copolymers of ethylene and α-olefin such as EPR. Based on this principle, we improved the mixing technique to control the distribution of MWCNTs in immiscible blends with a sea-island structure.

In this research, a blend of PP and EPR was employed as it is one of the most important immiscible blends used in industrial applications. We controlled the MWCNT distribution via the processing/mixing conditions, e.g., via the temperature and the nitrogen gas purging conditions. Our experimental results provide a method to effectively enhance the rigidity via the selective localization of MWCNTs in the matrix phase.

2. Experimental Section

2.1 *Materials*

The polymers used in this research were commercially available isotactic polypropylene PP (J108M, Prime Polymer, Japan) and ethylene-co-propylene rubber EPR

(EP11, JSR, Japan). The stereoregularity of PP is 96% (*mmmm*%, a meso-pentad value). The melt flow rate of PP is 45 g/10min at 230 °C. The number- and weight-average molecular weights of PP, determined by size exclusion chromatography, are 3.6×10^4 and 2.5×10^5, respectively, versus a polypropylene standard. The ethylene content in EPR is 52 wt.%, and the Mooney viscosity $ML_{(1+4)}$ 100 °C is 40.

A composite with 20 wt.% multi-walled carbon nanotubes, i.e., PP/MWCNT, was kindly provided by Hodogaya Chemical Co., Ltd., Japan in pellet form. The MWCNTs (NT-7, Hodogaya Chemical, Japan) were produced by a catalytic chemical vapor deposition technique using a floating reactant method and subsequent thermal treatment up to 2600 °C [28,29]. The diameter of the MWCNTs ranged from 40 to 80 nm, and the length was between 10 and 20 μm with a density of 2300 kg/m^3.

2.2 *Sample preparation*

PP/MWCNT (80/20) was mixed with neat EPR at either 190 or 280 °C for 10 min with a blade rotation speed of 50 rpm with a weight ratio of 80/20, i.e., PP/MWCNT/EPR = 64/16/20. The temperatures were selected as the lowest and highest ones for conventional processing operations of PP. In order to prevent marked chain scission reaction, 5000 ppm of a thermal stabilizer, 2-(tert-butyl)-6-methyl-4-(3-((2,4,8,10-tetrakis(tert-butyl)dibenzo[d,f][1,3,2]dioxaphosphepin-6-yl)oxy)propyl)phenol (Sumilizer-GP, Sumitomo Chemical, Japan) was added to all samples. Furthermore, the effect of nitrogen N_2 gas purging on the structure was investigated. Additionally, a blend of PP/EPR with a weight ratio of 76/24 (= 64/20) was also prepared at 190 °C for 10 min with 5000 ppm of the thermal stabilizer (no N_2 gas).

All samples were compressed into flat sheets with a thickness of 1 mm using a laboratory compression-molding machine (Table-type test-press, Tester Sangyo, Japan) at 190 °C under 10 MPa for 3 min and subsequently cooled at 25 °C for 3 min.

2.3 *Measurements*

The quenched PP/MWCNT/EPR sheets were crushed into powder form using a cryogenic sample crusher (JFC-300, Japan Analytical Industry, Japan). The powder was packed in a metal mesh bag and then immersed in xylene at room temperature for three days. Thereafter, the insoluble part, which is the part remaining after the EPR extraction, was taken out and dried to quantify its weight. The collected solution was also dried to obtain the soluble part. The weight fraction of the soluble part *S* was calculated using Eq. (1):

$$S = \frac{w_i - w_f}{w_i} \times 100, \quad (1)$$

where w_i and w_f are the weights of the initial sample and dried insoluble one, respectively.

The molecular weight of the soluble part in 1,2,4-trichlorobenzene at 140 °C was measured by size exclusion chromatography (HLC-8321GPC/HT, Tosoh, Japan).

Rheological measurements for PP, EPR, PP/EPR and PP/MWCNT/EPR were carried out using a parallel-plate rheometer (AR 2000ex, TA Instruments, Japan) at 170 and 190 °C under an N_2 atmosphere. The diameter of the plates was 8 mm for the composites and 25 mm for the samples without MWCNTs. All samples were kept in the rheometer for 10 min prior to the measurements.

The morphology and localization of the MWCNTs in the PP/MWCNT/EPR blends were investigated using scanning electron microscopy (SEM) (S4100, Hitachi, Japan) and transmission electron microscopy (TEM) (JEM-2000FX, JEOL, Japan). For SEM observations, the sheets were cryofractured in liquid N_2 and etched with xylene at room temperature for 3 days to remove the EPR fraction on the surface of the blend. The etched samples were coated with Pt-Pd by a sputter coating machine prior to the observations. For

TEM, the sheets were prepared by cutting a cryosection using an ultra-microtome (MT-XL, RMC-Boeckeler, AZ, USA) with a diamond knife after exposure to ruthenium tetraoxide.

Electrical resistivity measurements were carried out on the surface of the compressed films using a constant-current supply resistivity meter (MCP-T610, Mitsubishi Chemical Analytech, Japan). The resistivity was measured five times for each sample at room temperature and the average value was calculated.

The temperature dependence of the dynamic tensile moduli was measured using a dynamic mechanical analyzer (Rheogel-E4000, UBM, Japan) at a heating rate of 2 °C/min over a temperature range from −80 to 160 °C. The applied frequency was 10 Hz.

Tensile tests were performed at room temperature using a universal tensile testing instrument (LSC-50/300, Tokyo Testing Machine, Japan) at a constant crosshead speed of 50 mm/min (strain rate of 0.1 min^{-1}) according to the ASTM D638 standard test method. The specimens were dumbbell shaped (ASTM D638-V) films with a thickness of 0.5 mm and had a gauge length of 10 mm.

3. Results and discussion

Fig. 1 shows the shear storage modulus G' and loss modulus G'' as a function of angular frequency ω for individual pure polymers and their blends at 190 °C. It was found that both moduli of EPR were significantly higher than those of PP because of EPR's longer relaxation time caused by its high molecular weight. The zero-shear viscosities of the polymers at 190 °C were 730 Pa s for PP and 45,000 Pa s for EPR. In the case of the PP/EPR blend, a long relaxation mechanism ascribed to the phase separation is clearly visible in the $G'(\omega)$ curve. This is a typical phenomenon observed for an immiscible polymer blend with high viscous dispersions in a low viscous matrix [30–32].

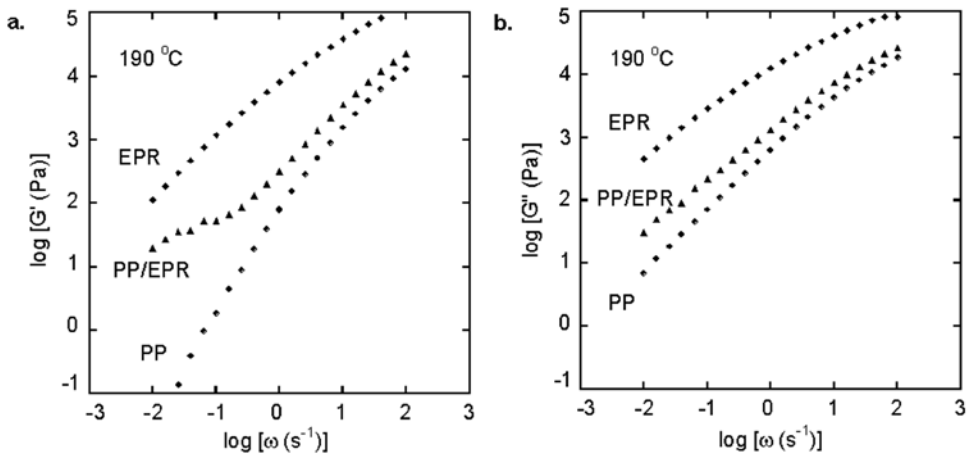

Fig. 1. Frequency dependence of oscillatory shear moduli such as (a) storage modulus *G′* and (b) loss modulus *G″* for PP, EPR and PP/EPR (64/20) at 190 °C.

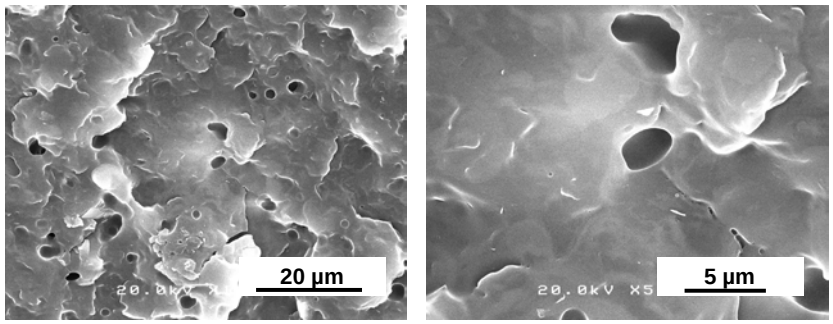

Fig. 2. SEM image of fractured surface of PP/EPR (64/20) after removal of EPR.

The morphology of the PP/EPR (64/20) blend was observed by SEM using the cryofractured surface as shown in Fig. 2. The EPR fraction was removed by xylene at room temperature. Prior to the experiment, it was confirmed that a pure EPR sheet is dissolved in xylene under the same experimental conditions. Fig. 2 shows the SEM image of the PP/EPR (64/20) blend. A sea-island structure in which EPR domains are dispersed in the PP matrix is clearly visible. It can be observed that the dispersed EPR domains are large and irregular in the shape owing to the long relaxation time of EPR.

PP/MWCNT and EPR were mixed at various conditions to establish a mixing technique to control the MWCNT distribution and thus the mechanical properties of the blend with MWCNTs. Besides, the effect of N_2 purging was also examined.

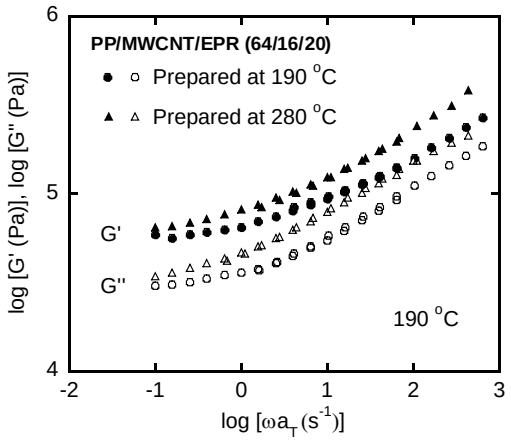

Fig. 3. Master curves of frequency dependence of oscillatory shear moduli for PP/MWCNT/ EPR composites prepared at 190 °C (circles) and 280 °C (triangle) without N_2 purging.

In Fig. 3, we demonstrated that both *G'* and *G''* of the composite prepared by mixing at 190 °C were higher than those of the composite prepared at 280 °C. Both samples were prepared without N_2 purging. The results suggest that the mixing temperature greatly affects the rheological responses, which is ascribed to the difference in the MWCNT distribution. Since the moduli of the sample prepared at the lower temperature are higher than those of the one prepared at the higher temperature, more MWCNTs could be distributed in the continuous phase, i.e., PP, when mixed at the lower temperature. We also found that the change in the shear moduli caused by the introduction of N_2 was barely detectable (data not shown here).

Although the rheological responses were similar irrespective of the N_2 purging, the surface resistivity was changed as follows; 12.2 Ω/sq. for the sample prepared at 280 °C without N_2 purging, 10.0 Ω/sq. for the sample prepared at 190 °C without N_2 purging, and

6.5 Ω/sq. for the sample prepared at 190 °C with N_2 purging, respectively. This difference is attributed to the MWCNT localization in the composite; when more MWCNTs reside in the PP phase, the conductive path builds up more easily in the matrix, leading to a low electrical resistivity. The present results suggest that the surface resistivity is more sensitive to the uneven distribution of the MWCNTs. Moreover, it should be noted that the N_2 purging enhances the MWCNT dispersion in the matrix to some degree.

Furthermore, the weight fraction of the insoluble part in xylene at room temperature was measured using the sample powder. It was found that the weight fraction of the composite prepared at the lower temperature with N_2 purging was 79.5 wt.%, which corresponds to the weight proportion of PP and MWCNTs in the composite. This demonstrates that most MWCNTs were located in the PP phase. When the sample was prepared without N_2 purging at 190 °C, it was 82.0 wt.%. For the composite prepared at 280 °C without N_2 purging, the weight fraction of the insoluble part was 87.7 wt.%, suggesting that the EPR was not dissolved completely in the solvent. This result indicates that undissolved EPR (7.7 wt.%) was adsorbed on the MWCNT surface.

The molecular weight of PP in the composites was measured using the soluble part in 1,2,4-trichlorobenzene at 140 °C. As shown in Fig. 4, the molecular weight and its distribution of the composite prepared at 280 °C without N_2 purging were almost the same with those of the PP/MWCNT, although the composite mixed at 190 °C with N_2 purging shows higher molecular weight due to the dissolution of EPR fraction. The result demonstrates that chain scission reaction of PP does not take place drastically even at 280 °C, presumably owing to a large amount of the thermal stabilizer.

To identify the MWCNT dispersion in the composite, SEM observations were performed using the composites prepared with different mixing conditions (Fig. 5).

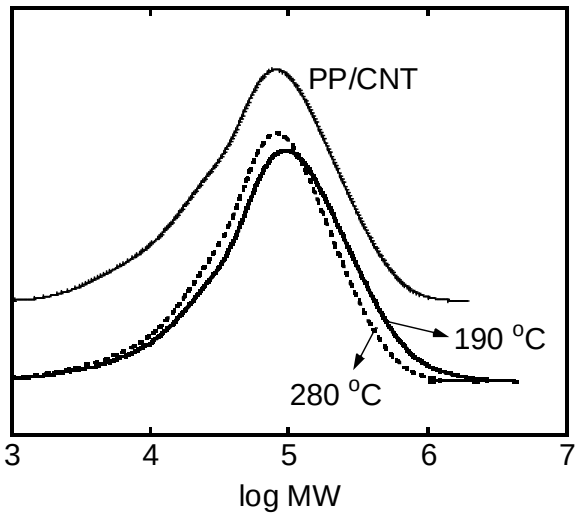

Fig. 4. Molecular weight distribution of soluble parts in 1,2,4-trichlorobenzene at 140 °C for PP/MWCNT (thin solid line) and PP/MWCNT/EPR composites prepared at 190 °C with N_2 purging (bold solid line) and 280 °C without N_2 purging (bold dotted line).

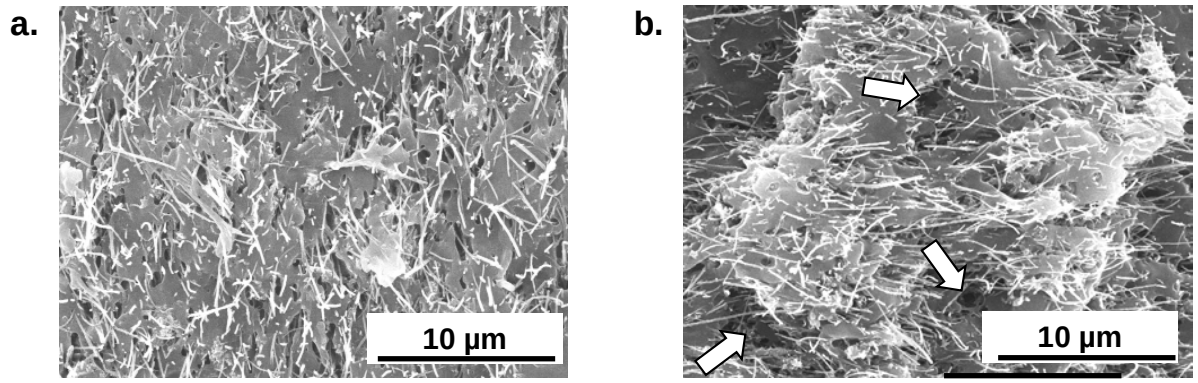

Fig. 5. SEM images of fractured surfaces of PP/MWCNT/EPR composites prepared at (a) 190 °C with N_2 purging and (b) 280 °C without N_2 purging. EPR fraction was removed by xylene prior to Pt-Pd coating.

Because the fractured sample was immersed in xylene, we attribute the holes detected in both samples to the dispersion pattern of EPR. Compared with the blend without MWCNTs (Fig. 2), the domain sizes of EPR were obviously small after the incorporation of the MWCNTs. Considering that MWCNTs were added in PP first, the fine dispersion of EPR

is attributed to the change in the viscosity ratio between PP and EPR. A fine dispersion is known to be obtained when the viscosity ratio is close to 1 [33,34]. In the composite prepared at 280 °C without N_2 purging, some large holes are detected, which are denoted by arrows, compared with that prepared at 190 °C with N_2 purging. Once the MWCNTs moved to EPR, the viscosity ratio increased significantly and therefore the morphology became coarse. The effect of the N_2 purging on the morphology was not detected by the SEM observation.

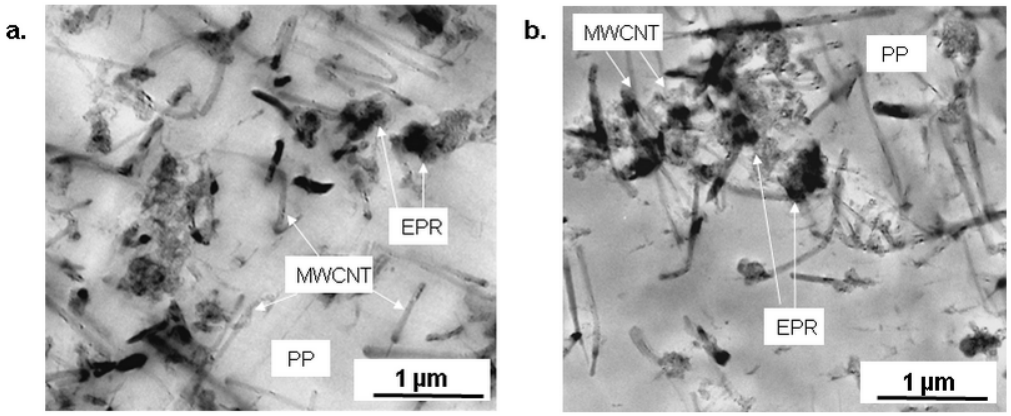

Fig. 6. TEM images of PP/MWCNT/EPR composites prepared at (a) 190 °C with N_2 purging and (b) 280 °C without N_2 purging.

The MWCNT dispersion was also examined via TEM. Fig. 6 shows TEM images of the PP/MWCNT/EPR composites. The grey continuous phase is PP, while the dark dispersed phase is EPR. As seen in the figure, more MWCNTs were localized in EPR when the sample was prepared at 280 °C without N_2 purging, which is in agreement with the conclusions drawn from the SEM images and solvent immersion experiments.

These results indicate that a large amount of MWCNTs are localized in the PP phase when PP/MWCNT/EPR was prepared at 190 °C with the introduction of N_2 gas. In contrast, the MWCNTs were transferred from PP into the EPR phase at the higher mixing temperature and distributed within it. The MWCNT migration occurs owing to the adsorption of EPR on the MWNCT surface at the high temperature, presumably with the aid of oxygen, which

promotes the generation of free radicals of the ethylene unit in EPR molecular chains [6,35,36].

Mechanical properties were evaluated to clarify the effect of the MWCNT localization. Temperature dependence of the tensile storage modulus *E'* and loss modulus *E''* for the neat PP/EPR and the PP/MWCNT/EPR composites that have different structures is shown in Fig. 7. The glass transition temperature T_g of each sample was obtained from the peak temperature in the *E''* curves and the results are listed in Table 1.

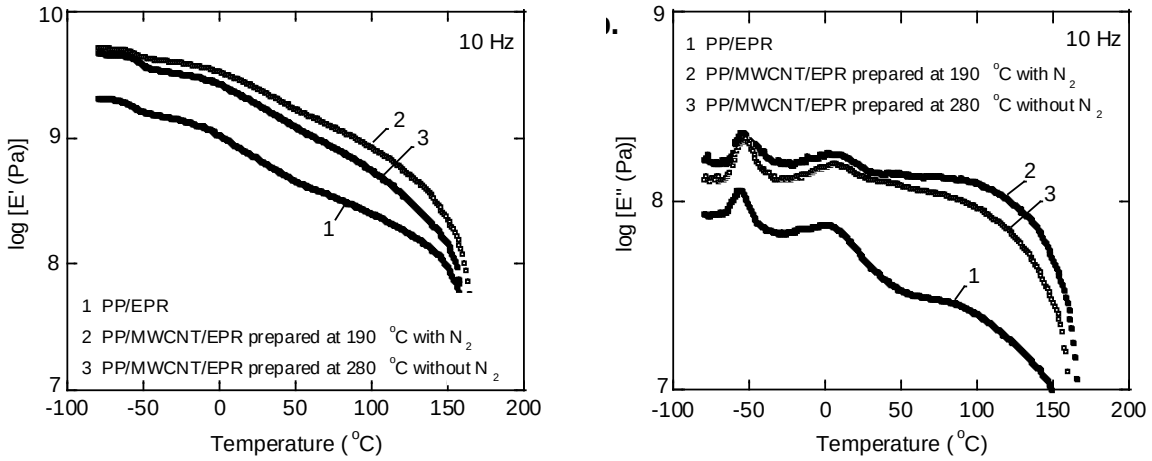

Fig. 7. Temperature dependence of (a) tensile storage modulus *E'* and (b) loss modulus *E''* for PP/EPR (1) and PP/MWCNT/EPR prepared by different mixing conditions (190 °C with N_2 purging (2) and 280 °C without N_2 purging (3)).

Table 1. Glass transition temperature of PP/EPR and PP/MWCNT/EPR

Samples	T_g (°C)	
	EPR	**PP**
PP/EPR	-56.1	4.8
PP/MWCNT/EPR prepared at 190 °C with N_2	-55.3	5.3
PP/MWCNT/EPR prepared at 280 °C without N_2	-52.3	5.4

We found that E' is greatly enhanced by the addition of MWCNTs owing to the filling effect of rigid materials [1,30,39], which was more pronounced for the composite prepared at 190 °C with N_2 purging. This is reasonable since more MWCNTs reside in the matrix. Moreover, all the samples show double peaks in the E'' curve, corresponding to the T_g values of the EPR and PP phases. As seen in Fig. 7(b), the T_gs of EPR and PP in the binary blend are −56.1 and 4.8 °C, respectively. We did the same measurements three times for each sample and confirmed that the difference among the samples is reproducible. Furthermore, the T_g of PP is shifted slightly to a higher temperature by the addition of the MWCNTs with an enhanced α relaxation mode. The well-developed crystalline structure, presumably caused by the nucleating ability of the MWCNTs [24,37,38], is responsible for both the prominent α relaxation mode as well as the T_g shift of PP (owing to the restricted motion of amorphous chains by crystals). Moreover, it should be noted that the T_g of EPR in the composite prepared at 280 °C without N_2 purging is located at a higher temperature than that of EPR in the PP/EPR blend without the MWCNTs. This is attributed to the reduced motion of the EPR molecules adsorbed on the surfaces of the MWCNTs. Finally, it should be noted that the storage modulus of the composite prepared at 190 °C with N_2 purging is greatly higher than that at 280 °C without N_2 purging in the wide temperature region. This result demonstrates that the rigidity is enhanced efficiently by the MWCNT localization in the matrix.

Fig. 8 shows the stress–strain curves. The tensile properties are summarized in Table 2. It is reasonably found that the PP/MWCNT/EPR composites show higher yield stress than the PP/EPR blend owing to the reinforcing ability of the MWCNTs, which is pronounced for the composite prepared at 190 °C with N_2 purging. This is plausible because the MWCNTs, which are dispersed in the matrix, enhance the stiffness with a consequent increase in the modulus. Further, it should be noted that the material shows a large elongation at break, demonstrating that the fracture energy is significantly larger than that of the composite

prepared at 280 °C without N_2 purging. When MWCNTs are located in the EPR phase, leading to the modulus enhancement of rubber dispersions, the reinforcing capability was greatly reduced. The result indicates that the enhancement of the tensile properties is dependent on the mixing condition.

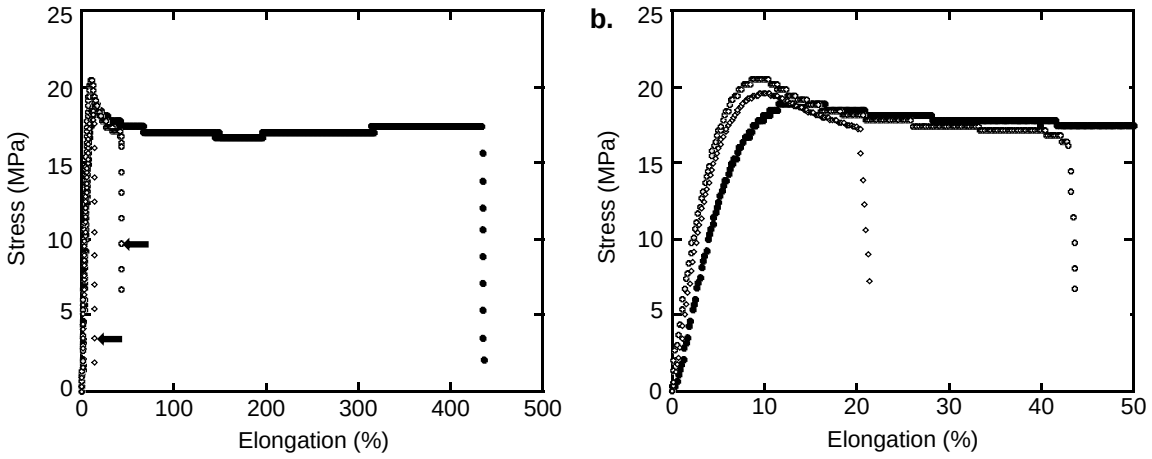

Fig. 8. Stress-strain curves for PP/EPR and PP/MWCNT/EPR prepared by different mixing conditions (190 °C with N_2 purging and 280 °C without N_2 purging). The initial parts in the small strain region are shown in (b).

Table 2. Tensile properties of PP/EPR and PP/MWCNT/EPR

Samples	Yield stress (MPa)	Elongation at break (%)
PP/EPR	18.6±0.3	487±65
PP/MWCNT/EPR prepared at 190 °C with N_2	20.6±0.8	47±10
PP/MWCNT/EPR prepared at 280 °C without N_2	19.5±0.3	20±5

Overall, the findings demonstrate that the localization of MWCNTs can be controlled mostly via the mixing temperature as presented in the PP/MWCNT/EPR composites. Moreover, mixing at 190 °C with the addition of N_2 purging was effective at controlling the preferential localization of the MWCNTs in the PP matrix of the PP/EPR blend with the sea-

island structure. This technique is available for other polymer blends, at least, those containing EPR as an impact modifier, because the adsorption of EPR molecules on the surface of the MWCNTs is responsible for making the localization of the MWCNTs in the rubbery phase. We also expect that this concept will widen material design possibilities to develop an advanced rubber-toughened plastic with high rigidity and high impact strength.

4. Conclusions

The effect of the mixing temperature along with the introduction of N_2 gas on the localization of MWCNTs in immiscible PP/EPR blends was studied. The results demonstrate that the MWCNTs were dispersed in the continuous PP phase when the composite was mixed at low temperature. Furthermore, N_2 purging was also effective to the preferential dispersion of MWCNTs in the matrix to some degree. When the mixing temperature was increased up to 280 °C without the use of N_2 gas, more MWCNTs were distributed in the dispersed EPR phase, which we attribute to the adsorption of EPR molecules on the MWCNT surface during melt mixing. As expected, when the MWCNTs were localized in the PP matrix, both the Young's modulus and yield stress were higher than those for the sample in which the MWCNTs were confined to the EPR phase. Moreover, the elongation at break was larger than that for the composite mixed at 280 °C without N_2 purging. The results prove that the rigidity of PP/EPR blends was improved by appropriate mixing conditions, i.e., at low temperature with the introduction of N_2 gas, because MWCNTs were selectively localized in the matrix.

Acknowledgement

This work was promoted by COI program “Construction of next-generation infrastructure system using innovative materials” – Realization of safe and secure society that

can coexist with the Earth for centuries – Supported by Japan Science and Technology Agency (JST).

References

[1] S. Iijima, Helical microtubules of graphitic carbon, Nature 354 (1991) 56-58.

[2] E. Logakis, C. Pandis, V. Peoglos, P. Pissis, C. Stergiou, J. Pionteck, P. Pötschke, M. Mičušík, M. Omastová, Structure–property relationships in polyamide 6/multi-walled carbon nanotube nanocomposites, J. Polym. Sci. Part B Polym. Phys. 47, (2009) 764-774.

[3] M.H. Al-Saleh, U. Sundararaj, Microstructure, electrical, and electromagnetic interference shielding properties of carbon nanotube/acrylonitrile–butadiene–styrene nanocomposites, J. Polym. Sci. Part B Polym. Phys. 50 (2012) 1356-1362.

[4] Y.P. Mamunya, Morphology and percolation conductivity of polymer blends containing carbon black, J. Macromol. Sci. B 38 (1999) 615-622.

[5] K. Prashantha, J. Soulestin, M.F. Lacrampe, P. Krawczak, G. Dupin, M. Claes, Masterbatch-based multi-walled carbon nanotube filled polypropylene nanocomposites: assessment of rheological and mechanical properties, Compos. Sci. Technol. 69 (2009) 1756-1763.

[6] R. Wiwattananukul, Y. Hachiya, T. Endo, S. Nobukawa, M. Yamaguchi, Anomalous transfer phenomenon of carbon nanotube in the blend of polyethylene and polycarbonate, Compos. Part B 78 (2015) 409-414.

[7] A.V. Doan, S. Nobukawa, S. Ohtsubo, T. Tada, M. Yamaguchi, Selective migration of silica particles between rubbers, J. Polym. Res. 20 (2013) 145-150.

[8] A. Göldel, A. Kasaliwal, P. Pötschke, Selective localization and migration of multiwalled carbon nanotubes in blends of polycarbonate and poly(styrene-acrylonitrile), Macromol. Rapid Commun. 30 (2009) 423-429.

[9] A.C. Baudouin, J. Devaux, C. Bailly, Localization of carbon nanotubes at the interface in blends of polyamide and ethylene–acrylate copolymer, Polymer 51 (2010) 1341-1354.

[10] P. Pötschke, S. Pegel, M. Claes, D. Bonduel, A novel strategy to incorporate carbon nanotubes into thermoplastic matrices, Macromol. Rapid Commun. 29 (2008) 244-251.

[11] L. Zonder, A. Ophir, S. Kenig, S. McCarthy, The effect of carbon nanotubes on the rheology and electrical resistivity of polyamide 12/high density polyethylene blends, Polymer 52 (2011) 5085-5091.

[12] M. Jaziri, N. Mnif, V. Massardier-Nageotte, H. Perier-Camby, Rheological, thermal, and morphological properties of blends based on polypropylene, ethylene-propylene rubber, and ethylene-1-octene copolymer that could result from end of life vehicles: Effect of maleic anhydride grafted polypropylene, Polym. Eng. Sci. 47 (2007) 1009-1115.

[13] N. Mnif, V. Massardier, T. Kallel, B. Elleuch, Effects of nanoparticle treatment and compatibilizers on the properties of (PP/EPR)/nano-$CaCO_3$ blends, Int. J. Mater. Form. 1 (2008) 639-643.

[14] M. Yamaguchi, Y. Irie, P. Phulkerd, H. Hagihara, S. Hirayama, S. Sasaki, Plywood-like structure of injection-moulded polypropylene, Polymer 51 (2010) 5983-5989.

[15] L. Moballegh, S. Hakim, J. Morshedian, M. Nekoomanesh, A new approach to increase toughness of synthesized PP/EPR in-reactor blends by introducing a copolymerization step under low ethylene concentration, J. Polym. Res. 22 (2015) 1-11.

[16] Y. Liu, M. Kontopoulou, The structure and properties of polypropylene and thermoplastic olefin nanocomposites containing nanosilica, Polymer 47 (2006) 7731-7739.

[17] M. Sumita, K. Sakata, S. Asai, K. Miyasaka, H. Nakagawa, Dispersion of fillers and the electrical conductivity of polymer blends filled with carbon black, Polym. Bull. 25 (1991) 265-271.

[18] M. Sumita, K. Sakata, Y. Hayakawa, S. Asai, K. Miyasaka, M. Tanemura, Double percolation effect on the electrical conductivity of conductive particles filled polymer blends, Colloid Polym. Sci. 270 (1992) 134-139.

[19] R. Uotila, U. Hippi, S. Paavola, J. Seppälä, Compatibilization of PP/elastomer/microsilica composites with functionalized polyolefins: Effect on microstructure and mechanical properties, Polymer 46 (2005) 7923-7930.

[20] G. Wu, S. Asai, M. Sumita, A self-assembled electric conductive etwork in short carbon fiber filled poly(methyl methacrylate) composites with selective adsorption of polyethylene, Macromolecules 32 (1999) 3534-3536.

[21] G. Wu, S. Asai, M. Sumita, Entropy penalty-induced self-assembly in carbon black or carbon fiber filled polymer blends, Macromolecules 35 (2002) 945-951.

[22] H. Yui, G. Wu, H. Sano, M. Sumita, K. Kino, Morphology and electrical conductivity of injection-molded polypropylene/carbon black composites with addition of high-density polyethylene, Polymer 47 (2006) 3599-3608.

[23] V. Haddadi-Asl, Morphology and properties of conductive carbon/polyolefins composite, Iran. Polym. J. 5 (1996) 75-86.

[24] M. Hemmati, A. Narimani, H. Shariatpanahi, A. Fereidoon, M. Ghorbanzadeh Ahangari, Study on morphology, rheology and mechanical properties of thermoplastic elastomer polyolefin (TPO)/carbon nanotube nanocomposites with reference to the effect of polypropylene-grafted-maleic anhydride (PP-g-MA) as a compatibilizer, Int. J. Polym. Mater. 60 (2011) 384-397.

[25] O. Meincke, D. Kaempfer, H. Weickmann, C. Friedrich, M. Vathauer, H. Warth, Mechanical properties and electrical conductivity of carbon-nanotube filled polyamide 6 and its blends with acrylonitrile-butadiene-styrene, Polymer 45 (2004) 739-748.

[26] S. Phromdee, P. Larjai, S. Tiptipakorn, S. Rimdusit, Development of electronic packages from polypropylene/ethylene-propylene rubber blends: A double percolation approach, J. Met. Mater. Miner. 24 (2014) 33-36.

[27] H. Yoon, K. Okamoto, M. Yamaguchi, Carbon nanotube imprinting on a polymer surface, Carbon 47 (2009) 2840-2846.

[28] Y.A. Kim, T. Hayashi, M. Endo, Y. Kaburagi, T. Tsukada, J. Shan, Synthesis and structural characterization of thin multi-walled carbon nanotubes with a partially facetted cross section by a floating reactant method, Carbon 43 (2005) 2243-2250.

[29] J. Chen, J.Y. Shan, T. Tsukada, F. Munekane, A. Kuno, M. Matsuo, T. Hayashi, Y.A. Kim, M. Endo, The structural evolution of thin multi-walled carbon nanotubes during isothermal annealing, Carbon 45 (2007) 274-280.

[30] Y. Niu, L. Yang, K. Shimizu, J.A. Pathak, H. Wang, Z. Wang, Investigation on phase separation kinetics of polyolefin blends through combination of viscoelasticity and morphology, J. Phys. Chem. B 113 (2009) 8820-8827.

[31] M. Yamaguchi, T. Yokohara, B.M.A. Mohd Amran, Effect of flexible fibers on rheological properties of poly(lactic acid), Nihon Reoroji Gakkaishi, 41 (2013) 129-135.

[32] J. Seemork, T. Sako, B.M.A. Mohd Amran, M. Yamagcuhi, Rheological response under non-isothermal stretching for immiscible blends of isotactic polypropylene and acrylate polymer, J. Rheology 61 (2017) 1-11.

[33] X.Q. Liu, W. Yang, B.H. Vie, M.B. Yang, Influence of multiwall carbon nanotubes on the morphology, melting, crystallization and mechanical properties of polyamide 6/acrylonitrile–butadiene–styrene blends, Mater. Design 34 (2012) 355-362.

[34] J.P. Cao, J. Zhao, F. You, H. Yu, G.H. Hu, Z.M. Dand, High thermal conductivity and high electrical resistivity of poly(vinylidene fluoride)/polystyrene blends by controlling the localization of hybrid fillers, Compos. Sci. Technol. 89 (2013) 142-148.

[35] A.J. Peacock, Handbook of polyethylene structure, properties, and applications, Marcel Dekker, New York, 2000.

[36] M. Siriprumpoonthum, S. Nobukawa, Y. Satoh, H. Sasaki, M. Yamaguchi, Effect of thermal modification on rheological properties of polyethylene blends, J. Rheol. 58 (2014) 449-466.

[37] L. Valentini, J. Biagiotti, M.A. Lopez-Manchado, S. Santucci, J.M. Kenny, Effects of carbon nanotubes on the crystallization behavior of polypropylene, Polym. Eng. Sci. 44 (2004) 303-311.

[38] B.P. Grady, Carbon nanotube-polymer composites: maufacture, properties, and applications, Wiley, Hoboken, 2011.

[39] R. Wiwattananukul, Y. Hachiya, S. Nobukawa, M. Yamaguchi, Selective localization of carbon nanotubes in PC/PET blends, Polym. Comp. 2015; in press. DOI: 10.1002/pc.23672